Computational Approach of Dielectric Permitivities in $BaTiO_3$–Epoxy Composites

L. RAMAJO,* M. REBOREDO, D. SANTIAGO AND M. CASTRO
Institute of Research in Materials Science and Technology (INTEMA) (CONICET – National University of Mar del Plata), Juan B. Justo 4302 (B7608FDQ) Mar del Plata, Argentina

D. RAMAJO
International Center for Computer Methods in Engineering (CIMEC, INTEC) Güemes 3450 (S3000GLN) Santa Fe, Argentina

ABSTRACT: A numerical approach using a finite element method (FEM) was performed in order to determine the dielectric constant (ε') of $BaTiO_3$–epoxy composites. In order to diminish computational resources and analyse simple models, composite topology was represented by periodic structures based on FCC configurations, but introducing novel packaging protocols, defining the way composites are filled as particle concentration is increased. The dielectric response of these anisotropic and periodic structures was mathematically represented through a quasi-static approximation using the Laplace equation. The amount of inclusions was varied in order to represent diluted and concentrated systems and structures were assessed for the whole feasible range of volume fractions. The numerical results were compared with experimental data concluding that only packaging protocols that consider higher particle–particle interaction are suitable to represent the dielectric behavior of concentrated-composite materials.

KEY WORDS: polymer matrix composites, dielectric, finite element analysis.

INTRODUCTION

PREDICTION OF THE dielectric permittivity of composite materials can be very important in many relevant technological applications. In this way, theoretical models have been developed for two-phase composites (a substrate with particles) [1,2]. Some of the more well-known are serial, parallel, modified Lichtnecker's models, and the Maxwell–Wagner's equation. The serial and parallel models represent the

*Author to whom correspondence should be addressed. E-mail: lramajo@fi.mdp.edu.ar
Figures 1, 7 and 8 appear in color online: http://jcm.sagepub.com

0021-9983/08/00 0001–11 $10.00/0 DOI: 10.1177/0021998308094543

Los Angeles, London, New Delhi and Singapore

extreme cases where the material is composed of alternate layers of different phases, located normal or parallel to the applied field, respectively. On the other hand, Maxwell's equation deals with the dielectric constant of composites with spherical inclusions in a continuous matrix and Lichtnecker's model represents a widely used empirical relationship that does not consider any physical geometry characteristic of the composite material [3].

Although these models are currently used, they fail to get a fitting in the whole particle-concentration range. For this reason, many researchers have started to develop novel models based on numerical methods [2,4–6]. The aim of these methods is to obtain an estimation of the electric field distribution inside the composite material and to get the overall dielectric properties by post processing. A variety of methods have been employed to find the field problem in 2D and 3D domains. Examples of these are the boundary integral method [5], the finite element method (FEM) [2], and the finite-difference time-domain method [6]. Some advantages of FEM over the other methods are its potential to handle complex geometries by using unstructured meshes, its capability to consider non-homogeneous and non-linear material properties, and the feasibility to incorporate a large number of components. For these reasons, FEM seems to be a suitable way to obtain accurate descriptions of the electric field inside composites. Thereby, the main composite characteristics such as the dielectric properties of the phases and their concentrations and the size and distribution of particles play a crucial role by modelling composite materials by FEM.

It is clear that the most accurate numerical approach will be obtained by considering a computational domain size equal to the real sample and also taking into account the real particle-size distribution along with a random spatial distribution for particles. Nevertheless, such numerical 'random' models require higher computational resources. Also, the subtleties of the proper treatment of anisotropic and non-homogeneous properties is still not comprehensively understood and simulation of random hetero-structures is a field still in its infancy. Therefore, simplified periodic models must be employed.

As previously reported [7], for higher particle concentrations with very different dielectric properties for matrix and inclusions, the simplest periodic structure FCC is no longer appropriate to reproduce the particle distribution inside the composite. In such periodic structures, the particle–particle separation diminishes slowly while the particle concentration grows. In consequence, the particle–particle effects are scarcely taken into account. It is easy to note that a local concentration of particles will generate preferential paths, canalizing the electric field flow and affecting the dielectric response of the overall composite. For this reason, modeling dielectric properties of random composites entail the use of more complex periodic structures, involving lower computational requirements for their resolution. Of course, these structures must be considered as intermediated step before tackle the simulation of random configurations, which require higher computational resources [8,9].

In this work, 3D FEM is applied to calculate the dielectric permittivity (ε') of epoxy/$BaTiO_3$ composites using periodic structures based on the FCC configuration but with three different packaging protocols; one simple FCC and two complex FCC structures (involving highest particle–particle interaction). Numerical results are confronted with experimental ones obtained from samples prepared by the dipping technique using different $BaTiO_3$ concentrations.

FINITE ELEMENT METHOD

The dielectric permittivity of an homogeneous material can be obtained by solving Laplace's equation:

$$\nabla(\varepsilon \nabla \mathrm{u}) = 0 \quad \text{in } \Omega, \tag{1}$$

where u is the potential distribution inside a spatial domain Ω with a null charge density at all points. Starting by multiplying Equation (1) with an arbitrary residual function w and later integrating it by parts over Ω and then applying Green's theorem, it is possible to write Equation (1) as [9]:

$$\int_{\Omega} (\nabla^2 u) w \, \mathrm{d}\Omega - \int_{\Gamma_2} \{(q - \bar{q})w\} \, \mathrm{d}\Gamma + \int_{\Gamma_1} \left\{ (u - \overline{u}) \frac{\partial w}{\partial \overrightarrow{n}} \right\} \mathrm{d}\Gamma = 0 \tag{2}$$

where q is the derivative of u with respect to the normal vector to the boundary Γ of Ω ($\partial u/\partial \overrightarrow{n}$). The boundary Γ can be divided in two parts, Γ_1 and Γ_2 $\Gamma = \Gamma_1 \ \Gamma_2$). Expression (2) satisfies the differential Equation (1) inside the domain Ω for two types of boundary conditions; the Dirichlet boundary conditions $u = \bar{u}$ on Γ_1 and the Neumman boundary conditions $q = \bar{q}$ on Γ_2. If the function u exactly satisfies the Dirichlet boundary conditions, which means $u = \bar{u}$ on all Γ, then a weak formulation [9] can be used, integrating the first term of Equation (2) by parts over the domain Ω and then introducing the boundary conditions, as:

$$\int_0^1 \left\{ -\frac{\mathrm{d}u}{\mathrm{d}x} \frac{\mathrm{d}w}{\mathrm{d}x} w \right\} \mathrm{d}x = -[qw]_{x=0} + [qw]_{x=1}. \tag{3}$$

The $\bar{u}$ solution in engineering applications can be approximated by using u and w functions, by defining an approximate solution rather than an exact one. That is, u and w as a linear combination of N polynomial interpolation functions (ϕ_j) that represents the solution of u in Ω, from a discrete solution u_j in some specific positions. For this purpose, the FEM implementation consists of selecting an appropriate polynomial interpolation function for w, dividing the spatial domain Ω in cells, and applying Equation (2) in each one of them in order to calculate the nodal values u_j. These values must match the imposed boundary conditions over the boundary domain and give a solution for u inside the whole domain by using the interpolation functions. Finally, from the integral Equation (3) it is possible to build a non-linear matrix equation system, which is numerically solved applying an iterative method.

On the other hand, the effective permittivity ε, along the direction corresponding to the applied electric field can be calculated using the relationship [2]:

$$\int_S \varepsilon_i \left(\frac{\partial u}{\partial n} \right)_i \mathrm{d}s = \varepsilon \frac{U_2 - U_1}{e} (S_1 + S_2) \tag{4}$$

where V_2–V_1 denotes the potential difference imposed in the z direction (see Figure 2), e is the composite thickness in the same direction, ε_i is the permittivity of the surface where the field is applied, and S is its corresponding area.

COMPUTATIONAL PROCEDURE

As previously mentioned, simulation of the full geometry samples involves high computational requirements, so a representative fraction of the total volume was modeled. The cell volume $\Delta\Omega$ was filled with spherical inclusions of $BaTiO_3$ located in such a way to get a faced-centred cubic cell (FCC) distribution. Based on the FCC distribution three different strategies were considered in order to reach the maximum particle volume fraction:

1. FCC-S. It considers that all particles in the FCC arrangement grow simultaneously. The maximum particle diameter ϕ_{max} is limited by geometrical restrictions to $\sqrt{2}L/2$ ($\phi_{max} \approx 0.707$ L), where L is the cell size. It is due to the assumption that neither of the particles can penetrate inside the others [7].
2. FCC-ED1. In this configuration only the eighth part of the whole FCC cell has been considered. Figure 1 (left) indicates (by means of numbers) the sequence followed in this protocol to introduce the particles while the volume fraction of $BaTiO_3$ is increased. At first, a particle is placed at the cell corner (position 1). As long as particle volume fraction increases, the particle grows until it reaches the maximum particle diameter ϕ_{max}. After that, a second particle starts to grow in position 2 at the cell. The process continues until the maximum particle volume fraction ($\approx$ 0.74 for FCC structures) is reached.
3. FCC-ED2. As in the FCC-S configuration, in this case the whole FCC cell has also been evaluated. Here particles are placed following the sequence indicated in Figure 1 (right). As in the previous case, each particle grows until it reaches ϕ_{max} before a new particle is located in the next position. This methodology has the effect of filling the main packaging directions first.

The particle size was varied in order to analyze a wide range of particle volume fractions for each one of the protocols. The applied boundary conditions for all the configurations were a potential difference ($\Delta V = U_2 - U_1$) of 1 V along the z direction

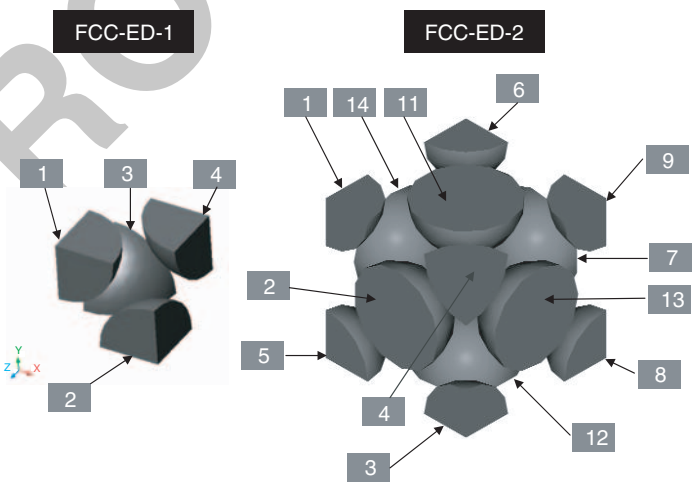

Figure 1. *Packaging configurations and the sequence they are generated. Left: FCC-ED1. Right: FCC-ED2 (geometrical restrictions to* $\phi_{max} = \sqrt{2}L/2 \approx 0.707L$*).*

(Dirichlet boundary condition) and gradients of potential equal to zero (Neumman boundary condition) for the others two Cartesian directions ($\partial u/\partial n_x = 0$ and $\partial u/\partial n_y = 0$), as shown in Figure 2.

Simulations were performed using software developed by the authors, while post processing of results was carried out with Matlab 5.0.

EXPERIMENTAL PROCEDURE

Samples were made of epoxy DER 325 (Dow Chemical) and DEH 324 (Dow Chemical) as the curing agent (12.5 phr) for the host matrix and commercial $BaTiO_3$ (TAM Ceramics Inc.) as the discrete phase with filler fractions from 0 to 65 vol% for the experimental mesurements. The epoxy and $BaTiO_3$ dielectric constants were 4.55 and 2400, respectively [7]. These parameters were determined at 30°C and 2500 Hz. The particle sizes of $BaTiO_3$ corresponing to 20, 50 and 80vol% were 0.6, 1.4, and 2.6 μm. The mixture viscosity was reduced by adding tetrahydrofuran (THF, Dorwil Chemical) with a concentration of 60wt%. The starting materials were mechanically mixed at 2000 rpm for 3–5 min.

The films were deposited through the dipping technique (rate of 3 cm/min) onto a glass substrate containing gold electrodes previously deposited by dc-sputtering. Finally, the deposited films were cured at 100°C for 2 h. In order to determine the $BaTiO_3$ concentration of composites each of them was analyzed by thermal gravimetric technique (TGA, Shimadzu TGA-50) in a controlled nitrogen atmosphere, starting from room temperature and heating up to 800°C at a rate of 10°C/min. Volume fraction was calculated using Equation (5) from the residual weight fraction obtained by TGA (see Figure 3):

$$BaTiO_3\ \text{vol\%} = \frac{(BaTiO_3\ \text{wt\%}/\rho_{BaTiO_3})}{(BaTiO_3\ \text{wt\%}/\rho_{BaTiO_3}) + (\text{epoxy wt\%}/\rho_{\text{epoxy}})} \tag{5}$$

where ρ_{BaTiO_3} is the filler density (5.84 g cm^{-3}) and ρ_{epoxy} is the matrix density (1.12 g cm^{-3}).

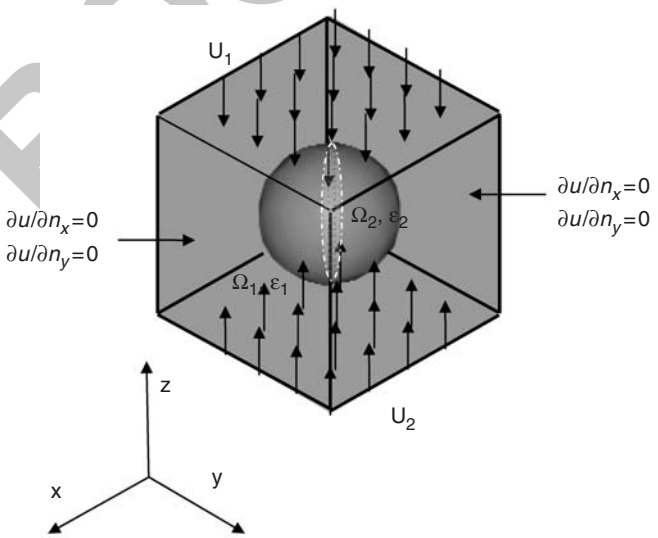

Figure 2. *Boundary conditions applied over the computational domain.*

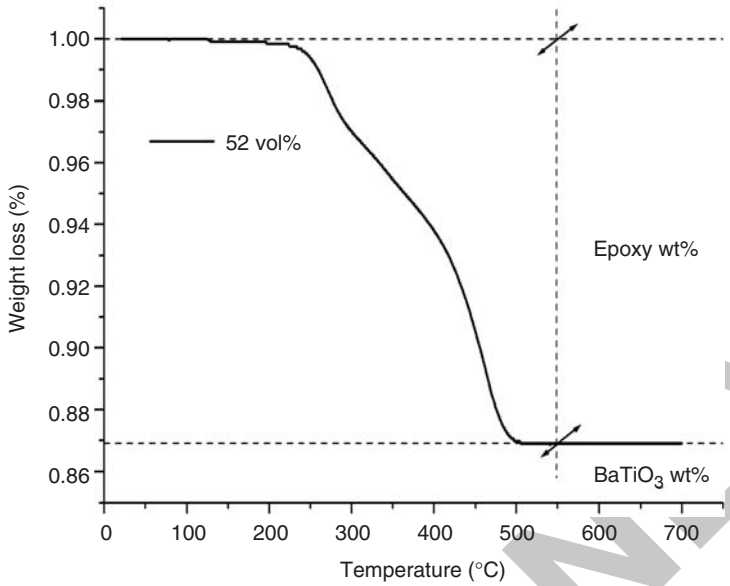

Figure 3. *Thermal gravimetric analysis (TGA) of composites with 52 vol% of $BaTiO_3$.*

The dielectric measurements were performed using a Hewlett Packard 4284A impedance analyzer in the frequency range of 20 Hz to 1 MHz at 30°C. Particle dispersion was studied using a scanning electron microscopy (SEM, JEOL 6460LV).

RESULTS AND DISCUSSION

The modified Lichtnecker's model expression is introduced in Equation (6):

$$\log\ \epsilon_c = \log\ \epsilon_M + V_2(1-k) \quad \log\left(\frac{\epsilon_p}{\epsilon_M}\right) \tag{6}$$

where V_2 is the filler volume fraction and ϵ_c, ϵ_M, and ϵ_p are the composite, matrix, and filler permittivities, and k is a constant ($k = 0.3$), respectively [10].

The effective-dielectric permittivity from FEM along with experimental data and modified Lichtnecker's model results are shown in Figure 4. Both the three packaging structures (FEM results) and Lichtnecker's model give acceptable predictions at low volume fractions. Nevertheless, simplest structure (FCC-S) cannot represent the composite behavior beyond 25 vol% particle concentrations, while empirical Litchnecker's model shows a tendency to fit experimental data, for low and intermediate particle concentrations.

As was previously reported [7], for intermediate particle concentrations the FCC-S does not take into account the particle–particle interaction in a correct form, leading to inaccurate results.

As regards the FCC-ED (FCC-ED1 and FCC-ED2) packaging structures, results are greatly improved with respect to FCC-S. It suggests that they are more suitable to represent the real composite topology.

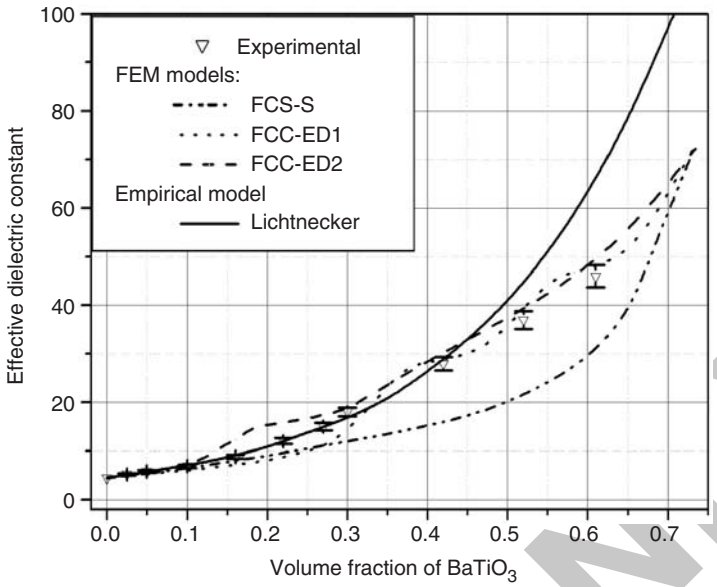

Figure 4. *Experimental results at 30°C and 2500 Hz, the Lichtnecker's model and FEM predictions from FCC-S, FCC-ED1, and FCC-ED2 cell configurations.*

Figure 5 shows the microstructure of composites with 20–50 vol% of particles. It is observed that particle distribution is almost homogeneous with trials of agglomeration and microporosity and zones without particles. In this way, composites with lower particle concentration present large zones without polymer along with particle-agglomeration zones. It is not so easy to find an appropriated periodic structure with a unique particle size which represents the topology of real composites. As was mentioned, the dielectric properties of matrix and inclusions are very different. Permittivity of $BaTiO_3$ is higher than the epoxy one (almost 530 times) indicating that the relation between the volume fraction of particles and the cumulative particle path, CPP (summit of particle diameters in function of the particle volume fraction) may contribute to understanding why results are dependent on the particle distribution protocol. Figure 6 shows the cumulative particle path vs the volume fraction for the three analyzed structures. Each abrupt step in the curves for FCC-ED1 and FCC-ED2 points out the incorporation of a new particle in the cell. Furthermore, the CPP obtained as the average of 40 random distributions is also included. Random cases were generated by using a homogeneous distribution to get the particle position (inside a three-dimensional unit cell) and a normal distribution (with a mean diameter of $0.707L$ and a dispersion of 35%) to obtain the particle sizes. Although the CPP is an insufficient parameter to reflect the composite topology because it does not take into account particle-agglomeration effects among others, random points in Figure 6 are shown to be more related with results obtained using the FCC-ED structures than the FCC-S one. At the same time, FCC-ED structures are close to one other and both are closer to the random points than FCC-S.

Returning to Figure 4, the FCC-ED1 configuration achieves a good correlation with experimental data, although it shows underestimations in the range of 10–30 vol% of particles. Nevertheless, results improve from 36 vol% when the third particle

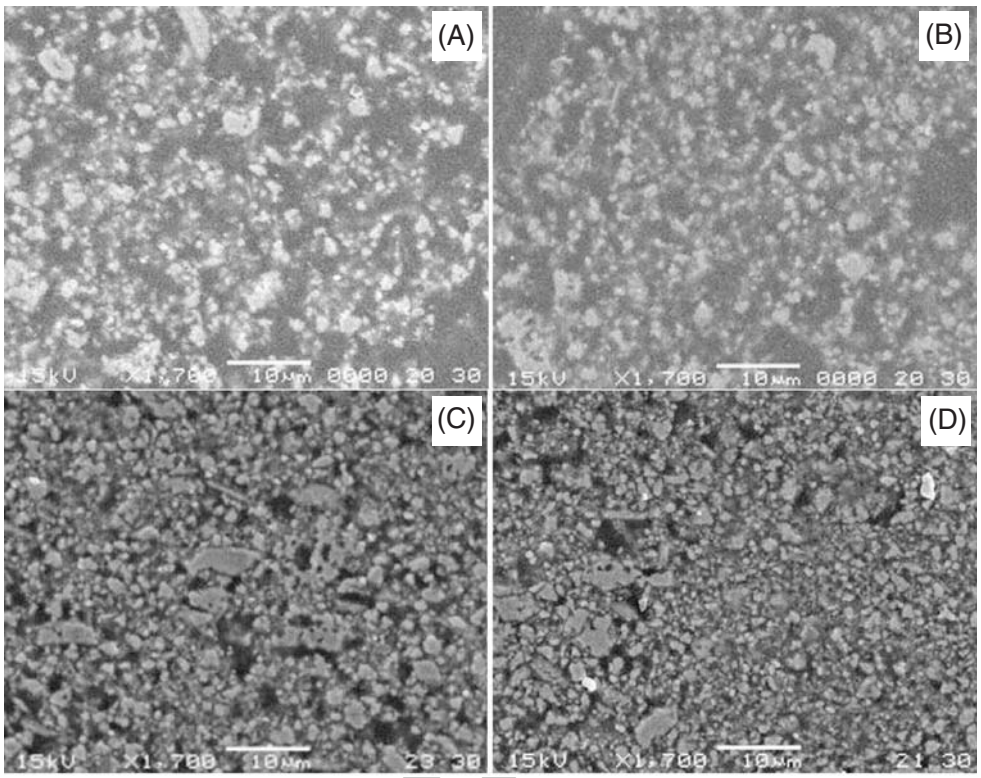

Figure 5. *SEM of composite samples with (A) 20, (B) 30, (C) 40, and (D) 50 vol%.*

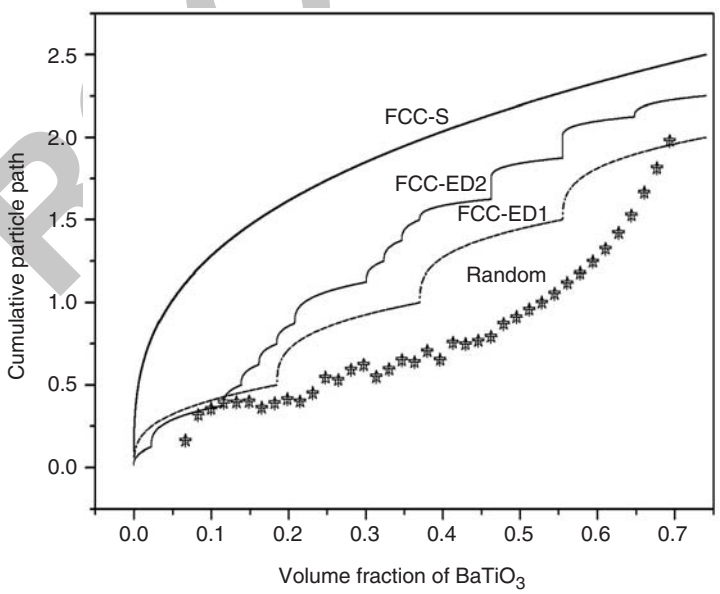

Figure 6. *Cumulative particle path estimation as a function of particle volume fraction.*

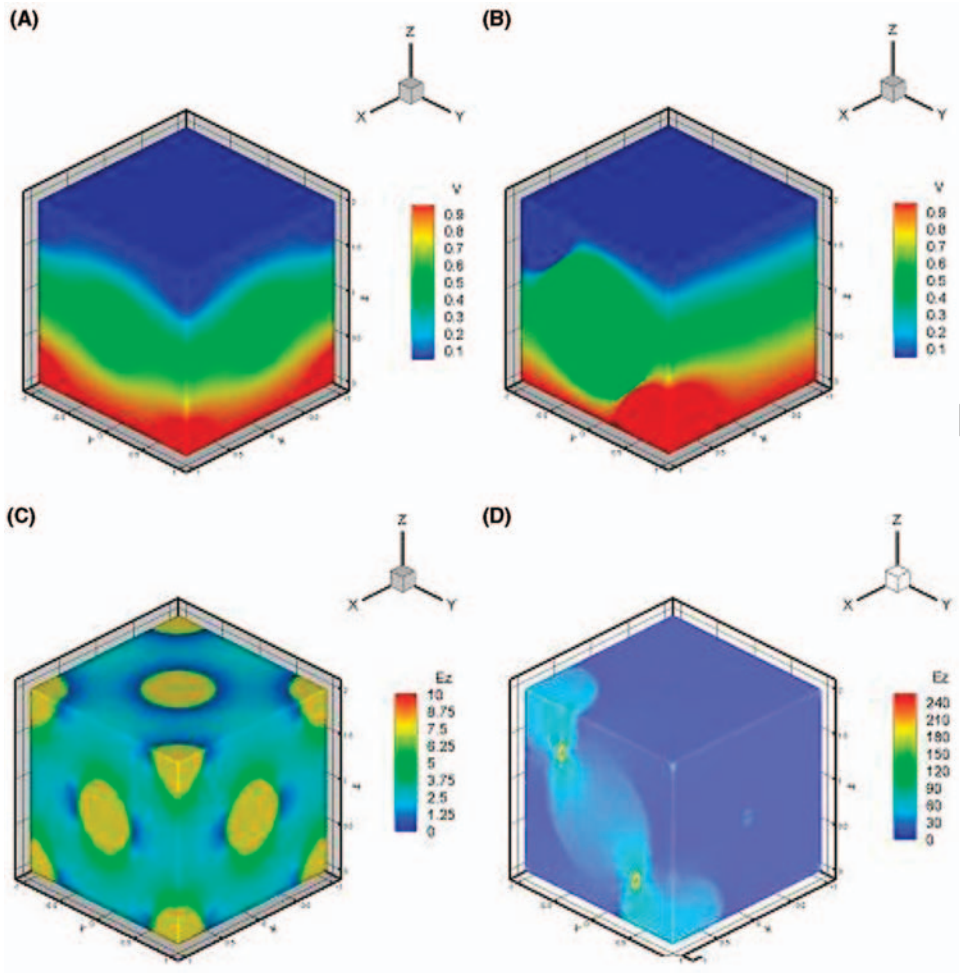

Figure 7. *FEM results obtained from FCC-S (A and C) and FCC-ED2 (B and D) of the potential difference (V) and the electric field (Ez) for a composite with 13vol% of particles.*

(see Figure 1, left) starts to grow and particle interaction becomes more relevant. As for the FCC-ED2, it gives smoother predictions. But, it also fails to predict correctly the range of particle concentration from 10 to 25 vol% overestimating the dielectric permittivity. This concentration range counts as a transition state where the composite is neither a diluted system nor a concentrated one. From Figures 1 and 6, it can be noted that particles 1–5 and 6–10 are located over planes parallel to the applied electric field. The greater CPP increment is observed while these planes are filled (volume fraction increasing from 0 to 36 vol%). This means that 60% of the total CPP is reached before volume fraction gets to 50 vol%.

Figure 7 shows results obtained from FCC-S and FCC-ED2 of the potential difference, V, and the electric field, Ez, for a composite with 13 vol% of particles. It can be noted that low particle interaction (FCC-S) produces low-intensity potential fields. On the other hand, for FCC-ED2, higher electric intensities are found even for relatively low volume fractions in regions where the interaction particle–particle reaches a maximum.

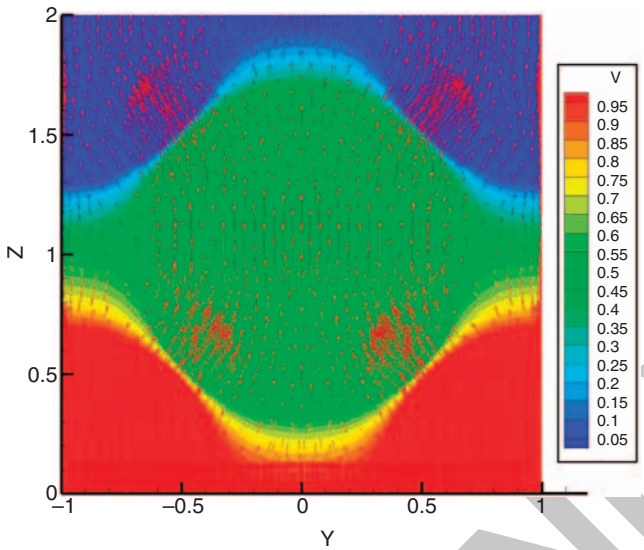

Figure 8. *Vector map of electric flow in a composite with 73 vol% of filler.*

This may explain why an overestimation on the permittivity values is obtained between 10 and 25 vol%.

Finally, in Figure 8 the electrical field on a body face for a composite FCC-ED2 with 73 vol% of filler is represented with vectors (Ey, Ez). It illustrates the effects of morphology over the potential gradients through the composite. As can be seen in Figure 8, the electric field flow turns to the particles following the easier path provided by them. Thus, if the particle–particle interaction increases, the electric field will grow and subsequently higher dielectric constants will be produced.

CONCLUSIONS

Numerical and experimental research about the dielectric response of epoxy/$BaTiO_3$ composites was carried out. Numerical simulations using FEM were confronted with the Lichtnecker's model, and experimental data. The following conclusions were reached:

- FEM results suggest that the electric field is strongly influenced by the relative position and distance between particles. In this way, the electric field distribution for volume fractions near to maximum-packaging threshold (≈ 0.74) presents higher interaction and corresponds to the highest dielectric constant values.
- The implemented numerical model reproduces the experimental behavior much better than the modified Lichtnecker's model. Both FCC-ED1 and FCC-ED2 show good agreement with experimental data, giving the latter a smoother response than the first one.
- The topology and the consequent dielectric response of highly concentrated composites could be represented by FCC-ED configurations, which consider higher particle–particle interaction than the simplest FCC-S.

- The cumulative particle path may be used as a useful parameter to compare, at least in a first step, different packaging protocols or random models. However, it does not take into account particle–particle effects or particle agglomeration.
- Finally, periodic structures based on a FCC configuration and a desirable packaging strategy can be used in order to represent composites with very different dielectric properties between the matrix and the inclusions.

ACKNOWLEDGMENTS

This work was supported by the National Council of Science and Technology of Argentina (CONICET). It was also achieved thanks to material donation from Dow Chemical Argentina due to management of Ariana Spinelli and Alfredo Fahnle.

REFERENCES

1. Uchino, K. and Takahashi, S. (1999). Dielectric Ceramic Materials. Ceramics Transactions, In: Nair and Bhalla (Eds), *The American Ceramic Society, Ohio*, **100**: 455–468.
2. Beroual, A. and Brosseau, C. (2001). *IEEE Trans. Dielectrics EI.*, **8**: 921.
3. Goodman, G. (1991). *Ceramic Capacitor Materials in Ceramic Materials for Electronics*, **2nd edn**, Marcel Dekker, New York.
4. Serdyuk, Y., Podoltsev, D. and Gubanski, S. (2005). *J. Electrostatics*, **63**: 1073.
5. Beroual, A. and Brosseau, C. (2003). *Progress in Materials Science*, **48**: 373.
6. Yoon, D.-H., Zhang, J. and Lee, B.I. (2003). *Materials Research Bulletin*, **38**: 765.
7. Ramajo, L., Ramajo, D., Santiago, D., Reboredo, M. and Castro, M. (2006). *Ferroelectrics*, **338**: 117.
8. Sanders, W.S. and Gibson, L.J. (2003). *Mat. Sci. Eng A*, **352**: 150–161.
9. Zinhiewicz, O.C. and Taylor, R.L. (1989). *The Finite Element Method*, MacGraw Hill Book Company, London.
10. Ramajo, L., Reboredo, M. and Castro, M. (2005). *Composites Part A*, **36**: 1267–1274.